Structure of SP-B/DPPC Mixed Films Studied by Neutron Reflectometry

W. K. Fullagar,* S. A. Holt,† and I. R. Gentle*
*School of Molecular and Microbial Sciences, The University of Queensland, Brisbane, Queensland 4072, Australia; and †ISIS Pulsed Neutron & Muon Source, Rutherford Appleton Laboratory, Chilton, Didcot OX11 0QX, United Kingdom

ABSTRACT The structures of films of pulmonary surfactant protein B (SP-B) and mixtures of SP-B and dipalmitoylphosphatidylcholine (DPPC) at the air/water interface have been studied by neutron reflectometry and Langmuir film balance methods. From the film balance studies, we observe that the isotherms of pure DPPC and SP-B/DPPC mixtures very nearly overlay one another at very high pressures, suggesting that the SP-B is being excluded from the film. The use of multiple contrasts with neutron reflectometry at a range of surface pressures has enabled the mixing and squeeze out of the DPPC and SP-B mixtures to be studied. We can identify the SP-B component of the interfacial structure and its position as a function of surface pressure. The mixtures are initially a homogeneous layer at low surface pressures. At higher surface pressures, the SP-B is squeezed out of the lipid layer into the subphase, with the first signs detected at 30 mN m^{-1}. At 50 mN m^{-1}, the subphase is almost completely excluded from the DPPC layer, with the SP-B content significantly reduced. Only a small amount of DPPC appears to be associated with the squeezed out SP-B.

INTRODUCTION

A wealth of experimental data concerning the pulmonary surfactant system has become available in recent years, with researchers using techniques as diverse as genetic mutation (1), fluorescence and Brewster angle microscopy (2), NMR (3), circular dichroism and infrared absorption (4), and x-ray reflectometry (5), prompting many reviews of the topic (6–8). The primary role of pulmonary surfactant is to enable the very low surface tensions necessary to prevent pulmonary collapse, although it may also have other functions (9) in addition to pulmonary defense (10). Four main proteins are associated with pulmonary surfactant, known as surfactant protein (SP)-A, SP-B, SP-C, and SP-D.

The hydrophobic SP-B and SP-C are of particular interest in the context of surfactant behavior and have been studied (6). SP-B is of primary interest because its deficiency can be fatal (11,12). Although SP-B is thought to mediate the transfer of lipids between the monolayer at the air/water interface and various structures in the alveolar fluid, the mechanism by which this is accomplished remains speculative. The primary structure of SP-B has been determined for several species and is well conserved among mammals. It is a small, homodimeric protein with dimeric molecular mass ~17.4 kDa, with each monomer consisting of 79 amino acids. A structure has been proposed for SP-B based on homologies with the protein NK-lysin (13), for which the NMR structure has been determined (14).

There has been considerable interest in the changes induced in surfactant phospholipid films by SP-B (as well as the smaller, even more hydrophobic peptide, SP-C) at the air/water interface. The surface activity of films of phospholipids mixed with SP-B have been studied by captive bubble methods (15), which demonstrated that SP-B facilitates rapid incorporation of lipids into the air/water interface and that the protein remains associated with the surface film. Langmuir trough measurements have also been reported on phospholipid/SP-B mixtures; results demonstrated evidence that the protein was lost from saturated lipid films at high surface pressures (16). More direct probes of structural changes induced by the surfactant proteins include scanning force microscopy after transfer to a solid support (17,18) and fluorescence microscopy or Brewster angle microscopy (19), among others. Another direct method that has not been applied to our knowledge is neutron reflectometry (NR). Although x-ray reflectometry studies of $SP\text{-}B_{1\text{-}25}$ were used to obtain structural information about the orientation of this model compound in monolayers of palmitic acid (5), we know of no similar studies to date of the native protein in monolayers of the primary pulmonary surfactant dipalmitoylphosphatidylcholine (DPPC) nor of any studies that have applied NR to such mixtures. Indeed, the only other related work in which NR has been applied in a similar way is that of Follows et al. (20), in which extracted samples of porcine and bovine lung surfactant dispersed in aqueous buffer were observed to form multilayer stacks at the air/water interface. Although not directly comparable to this work due to the very different nature of the samples (which, in their study, contain both SP-B and SP-C and associated lipids), our study demonstrates the power of NR to probe surface structure of complex biological film-forming materials.

This study includes two aspects: first, it extends previous investigations of the interfacial structure of SP-B on buffer solution as a function of surface pressure (21). These findings

Submitted March 28, 2008, and accepted for publication August 5, 2008.

Address reprint requests to Professor Ian Gentle, School of Molecular and Microbial Sciences, The University of Queensland Brisbane, Queensland, 4072 Australia. Tel.: 61-7-3365-4800; Fax: 61-7-3346-9960; E-mail: i.gentle@uq.edu.au.

W. K. Fullagar's present address is Chemical Physics, Chemical Center, Lund University, PO Box 124, SE-221 00 Lund, Sweden.

Editor: Jill Trewhella.

0006-3495/08/11/4829/08 $2.00

doi:10.1529/biophysj.108.134395

form the basis for the second aspect of the work, which is a study of mixtures of SP-B and DPPC on the same subphase.

MATERIALS

SP-B was isolated from cow lungs, as described previously (21), with the exception of the second chromatographic purification, which was carried out as described by Bünger et al. (22). In brief, fluid from lavaged lungs was centrifuged, and the pellet extracted into chloroform/methanol. The organic phase was evaporated to a few milliliters, applied to a Sephadex LH-20 column (Sigma-Aldrich, Sydney, Australia), and eluted with a 2:1 chloroform/methanol mixture. The first peak, monitored at 280 nm and containing the hydrophobic proteins and lipids, was dried and redissolved in chloroform/methanol. To separate the proteins and lipids, the mixture was eluted through a Vydac C4 preparative high-performance liquid chromatography column with 1:1 chloroform/methanol + 5% 0.1 M trifluoroacetic acid, and the first peak, containing the SP-B, was collected. The identity of the SP-B peak was confirmed by matrix-assisted laser desorption/ionisation-time of flight mass spectrometry.

Phospholipids were purchased from Avanti Polar Lipids (Alabaster, AL). To provide different contrasts for the NR measurements, either DPPC or chain deuterated (d_{62}) DPPC were used as appropriate, dissolved in a 4:1 chloroform/methanol (v/v) solvent mixture. Mixed films were produced by spreading from a single solution containing both lipid and protein in the appropriate proportions, determined as described in the Experimental section. The subphase was 0.1 M NaCl in either H_2O or D_2O with 0.01 M HEPES buffer and pH adjusted to 7.2. A buffer solution with a scattering length density of zero, the same as air, was made by mixing appropriate amounts of the two subphase solutions (air contrast-matched water [ACMW], $H_2O/D_2O \sim 92{:}8$).

EXPERIMENTAL

Surface pressure-area isotherms were recorded using a 600 cm^2 polytetrafluoroethylene (PTFE) Langmuir trough (NIMA Technologies, Coventry, UK) with a 1 cm chromatography paper (Whatman (Maidstone, UK) CR1) strip as the surface pressure sensing Wilhelmy plate. Isotherms were measured both independent of, and in conjunction with, the reflectometry measurements. Small volumes (typically $\sim$150 μL) of sample were spread dropwise onto the subphase surface, allowed to equilibrate for at least 5 min, then compressed to the desired surface pressure using a PTFE barrier. During reflectometry measurements, constant pressure was maintained using a feedback loop, although in general the films were quite stable over the course of the measurements. An antivibration table supporting the trough was activated during measurements.

Because the concentration of the SP-B solution was unknown before the NR experiments, the ratios for the mixed films were based on the isotherms of the pure components at 30 mN m^{-1} so that the coverage of the surface would be in the ratio of 2:3 (protein/lipid) at that pressure.

NR experiments were carried out using the CRISP time-of-flight reflectometer (23) at the ISIS spallation neutron source at Rutherford Appleton Laboratory, Didcot, UK. The reflectivity is measured as a function of momentum transfer, $Q = (4\pi/\lambda)\sin\theta$, where λ is the wavelength of the incident radiation and the angle of incidence, θ, was fixed at 1.5°. The reflectivity data were placed on an absolute scale after determination of the scale factor from a clean D_2O/air interface. Typical neutron measurements involved illumination times of $\sim$1 h, during which the isotherms indicated little loss of material from the interface. Films of SP-B were measured at surface pressures of 5, 15, 25, and 30 mN m^{-1}. We were unable to vary the contrast of the naturally derived SP-B molecule by deuteration, and so only the subphase and DPPC contrasts were varied. For the mixtures at each surface pressure measured (5, 20, 30, and 50 mN m^{-1}), three different contrast combinations were examined, which we denote A, B, and C throughout this work:

A = d_{62}-DPPC + SP-B on ACMW.
B = h-DPPC + SP-B on D_2O.
C = d_{62}-DPPC + SP-B on D_2O.

Data fitting programs based on the optical matrix formalisms (24,25) were used. The fitting depends upon parameterising the interface into one or more layers of material with interfaces whose shape is the convolution of the step function with a Gaussian function. The standard deviation of the Gaussian thus defines the interfacial roughness and is fixed at $\sigma = 3$ Å in the fits described here, which is a value comparable to the average amplitude of thermally excited capillary waves (26,27). In practice, the fits are not critically dependent on the roughness value chosen, and repeating the fits with a roughness of 6 Å (data not shown) has only a small effect on the fits and does not change the conclusions. Conversely, setting the roughness to 0 Å significantly changes the results. Our experience is that it is more reliable to use a constant value of 3 Å for liquid interfaces rather than to treat the roughness as a variable to be fitted. Simultaneous constrained refinement of the data collected with different contrasts was carried out. This fitting process reduces the number of models that adequately describe the data. The simplest possible model (a single layer) was examined first, with further layers added as required.

Subtraction of the appropriate contrast sets enables the volume fraction (V_f) of each component within a layer to be determined. For example, C − A, where the difference in signal is due to the change in subphase contrast, leads to the determination of the water density profile (and hence V_f) through the structure. Similarly, C − B leads to information regarding the lipid tail profile, providing the ability to determine the SP-B profile by subtraction of the volume fraction profiles from unity. The caveat on this approach is that two basic assumptions are required: first, the packing density and molecular arrangement are directly related to that of the pure compounds and, second, no account is taken of any hydrogen/deuterium exchange that will take place between the SP-B and the subphase (lipid headgroup exchange is well defined and can readily be calculated). For these reasons, the volume fraction analysis is most applicable to the upper layer, which has the lowest subphase content and where the conformation of the lipid tails and SP-B are most likely to be closest to the native state. The analysis gives particular insight into the pressure-dependent rearrangements that take place in this upper layer.

RESULTS AND DISCUSSION

This work follows our earlier study on the structure of films of pure SP-B at the air/water interface (21). It is important to note that the samples of purified SP-B were not dried after purification, and so it is difficult to accurately determine their concentration. This difficulty was overcome by the use of the unique ability of NR to measure surface concentration of films formed from our spreading solutions of pure SP-B, which allowed us to calculate the concentration and correct the isotherms. Before describing the work on mixed films, therefore, we discuss the reflectometry of the pure SP-B films.

SP-B reflectometry

The reflectivity and fitting from the protein prepared for this series of experiments is in agreement with those published previously (21), with the layer thicknesses within a few ångstroms of the reported values. This work concerns only bovine SP-B and includes data collected at one extra surface pressure, 25 mN m^{-1}. As is shown in Table 1, the data are fitted by a single-layer model at the lowest surface pressure, 5 mN m^{-1} and, similarly at 15 mN m^{-1}, there is no discernable improvement in fit quality with the application of a second layer. As the pressure is increased, the protein content of the layer increases, and the interface becomes more structured, such that at 25 and 30 mN m^{-1}, the data best fit a model with two layers extending a total of 50–60 Å into the solution, with the bottom layer containing a greater amount of subphase.

To analyze the scattering length density (SLD) values derived from the fitting procedure, knowledge of the scattering lengths of the various materials is required. Gaining this information is quite straightforward for DPPC and the subphases but somewhat more complicated for SP-B, because the protein sequence and the number of exchangeable protons needs to be known. The amino acid sequence of bovine SP-B has caused some controversy in the literature (28) owing to an early Edman degradation sequence (29) suggesting that it lacks several of the cysteine residues that have since been found to be critical to the tertiary and quaternary structure of the protein (30), as well as SP-B's intracellular trafficking during biosynthesis (1). In recent work, our group used a variety of techniques to determine the bovine SP-B sequence shown in Fig. 1. This sequence is in very good agreement with a bovine sequence presented previously (6) and is used in our calculation of the SP-B scattering length.

TABLE 1 Layer thicknesses for SP-B spread on pH 7.2 HEPES buffer

Pressure (mN m^{-1})	Layer 1 thickness (Å)	Layer 2 thickness (Å)	Area/SP-B (nm^2)	Protein at interface (mg)	Spreading solution (mg mL^{-1})
5	26 (1)	–	29 (2)	0.017 (1)	0.12 (1)
15	23 (1)	–	20 (1)	0.020 (2)	0.14 (1)
25	18.7 (7)	30 (1)	14.4 (7)	0.020 (1)	0.14 (1)
30	22.4 (5)	35 (1)	11.4 (4)	0.020 (1)	0.143 (9)

The calculated area per SP-B monomer and solution concentrations for the upper layer listed here have been calculated from the fits to the neutron reflectivity data.

If we use the fitted values as a guide and we repeat the analysis but arbitrarily fix the interfacial roughnesses at zero (thereby constraining all the material into the layer), the SLD and thickness values can be used to calculate the area per molecule. This method is straightforward when the subphase is ACMW (where the SLD equals zero) and, by definition, all scattering comes from the material spread at the interface. In other circumstances, allowance needs to be made for the contribution of the subphase to the scattering. The area per protein (A_p) is calculated using Eq. 1 for systems with an ACMW subphase as follows,

$$A_p = \frac{\sum b}{d \times SLD}, \quad (1)$$

where Σb is the sum of the scattering lengths of the individual atoms that make up the protein, and d and SLD are the fitted layer thickness and scattering length density, respectively. Because the trough area and the volume of solution are also known, the amount of material spread, and hence the concentration of the spreading solution, can be calculated for SP-B.

From the fits and application of Eq. 1, the area per protein, the amount of protein at the interface, and the concentration of the spreading solution were calculated (Table 1). It can be seen from the calculated values that the amount of material present at the interface is the same for the three higher pressures and slightly reduced for the lowest surface pressure. For consistency, it would be expected that the total amount present at the interface would be independent of surface pressure, assuming that the material is totally insoluble in the subphase. However, at the lowest surface pressure, the area per molecule is quite large, and the sensitivity of the techniques is at its worst. Despite this, the amount of material and the calculated solution concentration is almost within the error bars. The NR results enable calculation of the area per SP-B molecule. Fig. 2 shows the isotherm for SP-B corrected with the area per molecule calculated from the NR results. If the isotherm is compared with typical examples from the literature (16,22,31–33), it displays a similar shape and area per molecule.

SP-B/DPPC isotherms

Fig. 2 shows typical isotherms of SP-B, DPPC, and the mixed film. The SP-B solution concentration, determined above, was used to calculate a molar ratio of 46.2 DPPC molecules

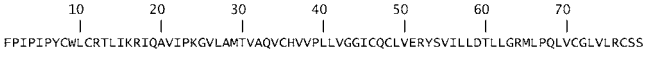

FIGURE 1 Confirmed bovine SP-B amino acid sequence used in SLD calculations.

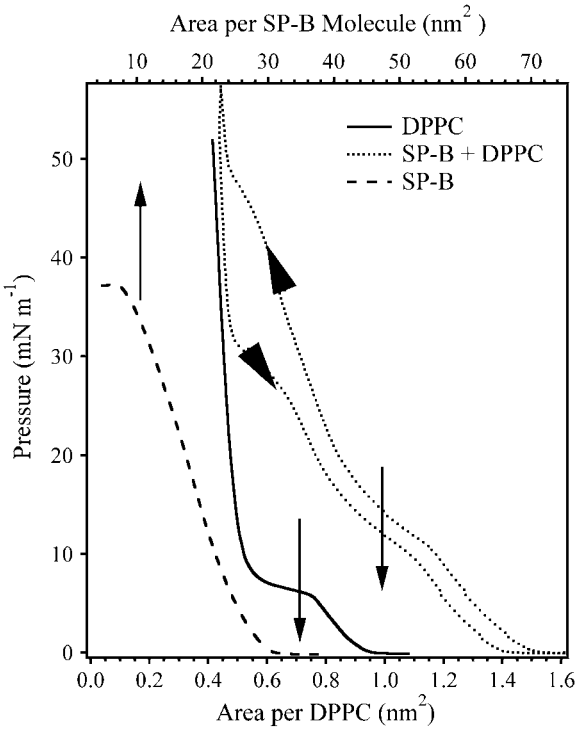

FIGURE 2 Pressure area isotherms of, DPPC, SP-B + DPPC mixture, and pure SP-B where the vertical arrows indicate the relevant molecular area axis. A compression and expansion trace is shown for the mixture, with the arrowheads showing the compression direction.

per SP-B monomer. The isotherms provide useful input to the constrained neutron refinements.

The isotherm of the mixture has been plotted as a function of the area per molecule of DPPC and shows some striking features. First, a phase transition similar to that observed for the lipid is still visible, but it is rather less distinct and shifted to noticeably higher surface pressure ($\sim$12 mN m^{-1}), whereas a second kink is observed at a higher pressure ($\sim$42 mN m^{-1}) Similar features have been observed previously (7,16). Second, when the surface pressure is above $\sim$50 mN m^{-1}, the isotherm of the mixture almost overlays the pure DPPC isotherm. This effect is even more pronounced when the initial region of the expansion section of the isotherm is considered. A straightforward interpretation of these results is that the nearly vertical region at high pressure corresponds to complete exclusion of SP-B and that, once this process is complete (that is, above $\sim$50 mN m^{-1}), the area and slope of the isotherm are determined by the material remaining at the interface, namely DPPC. For this interpretation to be correct, it is evident that no substantial quantity of DPPC is taken into the subphase during the squeeze-out of the protein. We note that, on expansion, the SP-B returns to the interface, with an initial region of hysteresis. It is quite remarkable, given the relative sizes of the SP-B and DPPC and much greater structural complexity of the protein, that it returns to the interface so quickly and apparently with a very similar area per molecule. Isotherm cycling (data not shown) reveals that there is little reduction in area on subsequent isotherms, indicating that the SP-B is readily incorporated back into the DPPC layer at low surface pressures and that any conformation variations on exclusion are reversible.

SP-B/DPPC reflectometry

Fig. 3 shows reflectivity data (*points*) and fits (*solid lines*) from the d_{62}-DPPC/SPB system at low and intermediate surface pressure on D_2O buffer (*a*) and ACMW buffer (*b*). The data sets with the higher surface pressure display greater variations from the Fresnel reflectivity profile than the lower pressure equivalents, indicating the development of interfacial structure with increased pressure. Fig. 4 displays the models used to obtain the fits in the form of SLD profiles as a function of depth. Data were fitted using a model with varying numbers of layers and a Gaussian roughness kept constant at 3 Å, smoothing the edges of the layers. The vertical lines in Fig. 4 are located at the center of the Gaussian interfacial roughness between each of the layers resulting from the fitting procedure, therefore indicating the positions of the boundaries between the layers. In the fitting of the three different contrast data sets, the layer thicknesses were constrained between each data set, because it is assumed that the physical dimensions of the films are unaffected by changes in deuteration of the components. The SLD profiles clearly show structural development at the interface as a function of surface pressure. All data sets were fitted with at least two layers, the basic interpretation being that the upper layer consisted predominantly of lipid tails/SP-B, the second layer was mainly lipid headgroups with some subphase, and, where required, a third layer of material squeezed out of the top layer. A two-layer model gives a good fit to data collected at 5 and 20 mN m^{-1}. Previously published x-ray (27) and neutron (34) reflectivity data on DPPC monolayers collected at surface pressures from 1.4 to 45.8 mN m^{-1} were also fitted with two-layer models, with the upper layer containing lipid tails and the lower layer containing lipid headgroups. Increasing the pressure to 30 and 50 mN m^{-1} requires the addition of a third layer (not seen in pure DPPC films) to give an acceptable fit. The thicknesses and SLD values of the resultant fits are shown in Table 2.

A comparison of the mixed-film SLD profiles (Fig. 4 and Table 2) with those from either of the components alone reveals a more complex interfacial structure for the mixture, particularly at high pressure. The form of the density profile is different at 30 mN m^{-1}, and the extent of penetration into the subphase is different ($\sim$60 Å for SP-B only and 75 Å for the mixture). This difference approximately corresponds to the expected thickness of the tail region of a DPPC monolayer, suggesting that the SP-B has been excluded from the film.

The interpretation of these results is aided by calculation of the V_f of each component, shown in Fig. 5. From the plot, it is quite clear that the proportion of water, DPPC tails, and SP-B in the upper layer remain virtually constant at the two lowest surface pressures. The initial response of the film to compres-

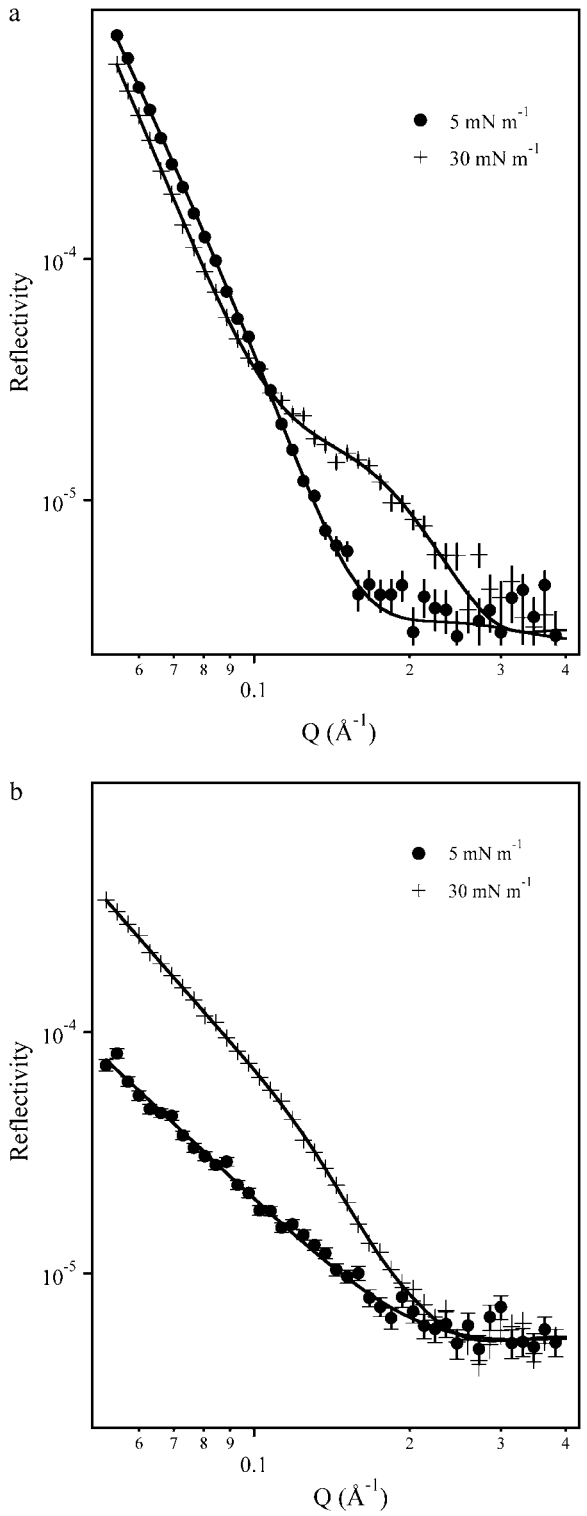

FIGURE 3 NR and fits for d-DPPC + SP-B mixtures on D_2O buffer (*a*) and ACMW buffer (*b*) where the symbols are the datapoints and the lines indicate the fit to the data.

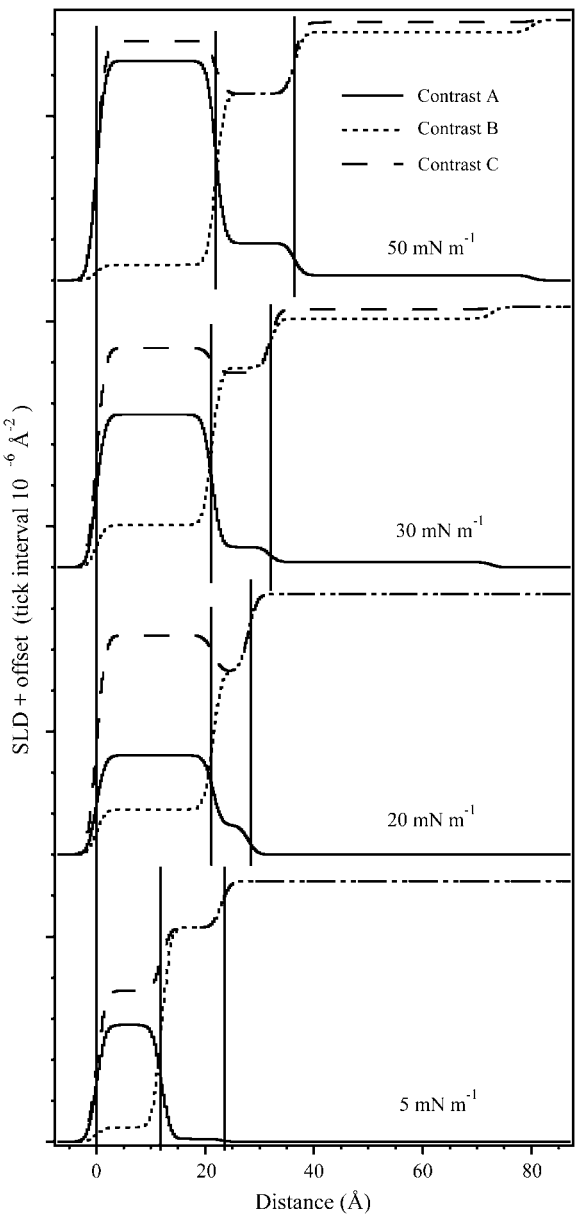

FIGURE 4 SLD profiles resulting from the constrained fitting of the three different contrast DPPC + SP-B data sets at four different values of surface pressure. The vertical lines indicate the boundaries between the fitted layers. In Results and Discussion, these are labeled layer one (5 mN m^{-1}), layers one and two (20 mN m^{-1}), and layers one, two, and three (30 and 50 mN m^{-1}) from left to right. Layer one is adjacent to air, and increasing distance implies a downward direction.

sion is a thickening, which is most likely driven by a reduction in the tilt angle of the DPPC tails. This thickening enables increased surface pressures without a change in film composition. Inspection of the V_f profiles reveals that the dominant change that takes place at surface pressure >20 mN m^{-1} is the exclusion of water from the film, with the V_f decreasing from $\sim$0.37 to 0.08. Simultaneously, the SP-B volume fraction decreases to 0.21, which is still quite high considering the surface

TABLE 2 Fitted parameters for mixed films of SP-B/DPPC with each of the three contrast combinations spread on pH 7.2 HEPES buffer

Contrast	Layer 1 thickness (Å)	SLD layer 1 /10^{-6} (Å^{-2})	Layer 2 thickness (Å)	SLD layer 2 /10^{-6} (Å^{-2})	Layer 3 thickness (Å)	SLD layer 3 /10^{-6} (Å^{-2})	χ^2
5 mN m^{-1}							
A	14.5	2.2	8.3	0.4	–	–	1.576
B	14.5	0.63	8.3	5.4	–	–	
C	14.5	4.0	8.3	5.4	–	–	
20 mN m^{-1}							
A	21.4	2.4	6.5	0.7	–	–	2.4295
B	21.4	1.1	6.5	4.5	–	–	
C	21.4	5.3	6.5	4.5	–	–	
30 mN m^{-1}							
A	20.8	3.9	9.2	0.46	42.9	0.13	1.1409
B	20.8	0.98	9.2	4.4	42.9	6.1	
C	20.8	5.5	9.2	4.4	42.9	6.3	
50 mN m^{-1}							
A	22.0	5.3	14.5	0.91	43.5	0.12	1.286
B	22.0	0.38	14.5	4.6	43.5	6.0	
C	22.0	5.8	14.5	4.6	43.5	6.3	

pressure and area per DPPC molecule (Fig. 2). This observation reveals that the condensed DPPC film can incorporate a significant amount of SP-B and retain its surface activity.

From the SP-B dimer structure proposed by Zaltash et al. (13), one can estimate a dimer volume of ~75000 Å^3. The spreading mixture contained 46.2 DPPC molecules per SP-B monomer. Therefore, taking a tail volume of 1026 Å^3 per DPPC molecule, the volume ratio of DPPC/SP-B would be 1.26. Fig. 5 also includes a trace representing the V_f ratio of DPPC/SP-B. At the lowest surface pressures, this value is in excellent agreement with that calculated above. At 30 and 50 mN m^{-1}, this ratio increases, indicating that the ratio of DPPC/SP-B in the upper layer has increased relative to the initial composition. This increase is readily explained by SP-B squeeze-out, which is also indicated by the third layer required for the fits. If SP-B and DPPC were squeezed out in the same ratio as initially spread, this line would remain constant.

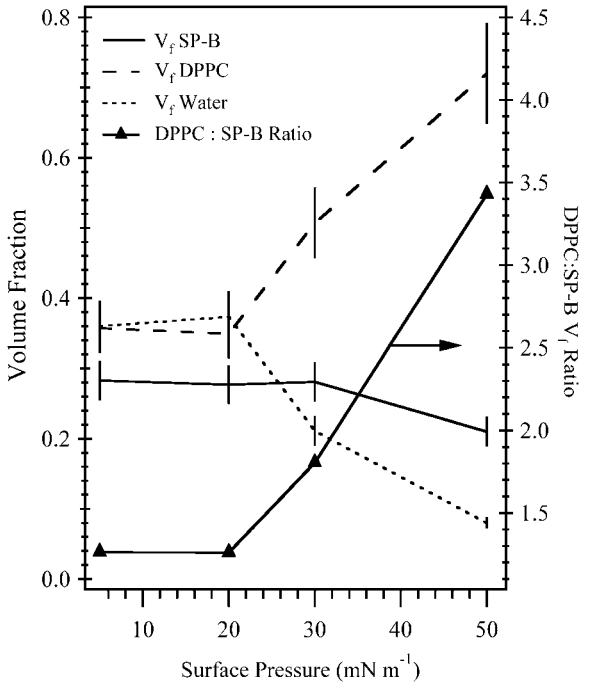

FIGURE 5 Volume fraction of film components in the upper layer (*lines*, *left axis*) and DPPC/SP-B V_f ratio (*line* and *markers*, *right axis*) as a function of surface pressure. The lines serve as a guide to the eye.

Layer three consists of material excluded from the upper layer at higher surface pressures. At 50 mN m^{-1}, this layer has a subphase V_f of 0.92, with the remaining 8% consisting of SP-B and DPPC. At this level, the material is at the detection limits of the experiment, and it is not possible to quantitatively determine the relative proportions of each component. From Figs. 4 and 5, one can draw some qualitative conclusions. As seen in Fig. 5, there is DPPC enrichment of the upper layer, and it is clear from Fig. 4 that layer three is not exclusively SP-B because there is a fitted SLD difference between contrasts B and C that could only be due to DPPC inclusion. That is, the SLD is lower for the mixture containing h-DPPC. Contrast A (containing d-DPPC) demonstrates that the DPPC content of the layer is quite low, because a significant DPPC incorporation would have resulted in a much higher fitted SLD.

As the surface pressure is further increased to 30 and finally 50 mN m^{-1}, the volume fraction of the dominant component in each layer increases, and the thicknesses are better defined, as shown by a decrease in the uncertainties of the fitted parameters. Data interpretation was tested by the selection of starting parameters to bias the fitting based on the following initial assumptions:

1. The initial parameters for the lower layer were selected to correspond to a layer of lipid tails. Under these conditions, one of two outcomes was observed: either the SLD refined to the form (seen in Fig. 4) or it remained near the starting position but altered the parameters of the other layers such that a poor fit to the data was achieved.
2. The SLD of the lower layer was fixed at a value representative of a mixed layer, which produced a poor fit with the program typically attempting to place two lipid-like layers with nonphysical thicknesses above the mixed layer.
3. Finally, we attempted to invert the layers, that is, the middle layer was made to be lipid tails, the lower layer the headgroup region, with the top layer assumed to be squeezed-out SP-B. This approach produced poor fits with nonphysical values for the fitting parameters.

We therefore conclude that the interpretation showing a squeezed-out SP-B layer below the DPPC with a layer containing lipid headgroups in between to be appropriate. Whereas SP-B is considered to be a very hydrophobic protein, it is not as hydrophobic as the aliphatic tail regions of DPPC. Pastrana-Rios et al. (35,36) have used external reflection Fourier transform infrared spectroscopy to study monolayers of SP-B and DPPC. Their work has demonstrated that SP-B is squeezed out of DPPC monolayers into solution, but they do not comment as to whether the protein is escorted by lipid. Taneva and Keough (16) concluded from surface pressure-area measurements that SP-B accompanied by a small amount of DPPC is excluded from mixed films at surface pressure >40 mN m^{-1}. This is qualitatively in agreement with this work, although comparisons are often complicated by variations in composition used by different authors. A dimer structure for SP-B squeezed out of monolayers of DPPC and DPPG (4:1 molar ratio) has been proposed (33) in which a positively charged α-helix face is presented to the solution with the more hydrophobic uncharged region of each monomer adjacent. This type of conformation would be quite stable in solution. A number of other authors have studied mixtures of DPPC and unsaturated lipids with SP-B derived from various sources, and it has been shown that SP-B resides in the fluid environments of such films (8) and that exclusion of both protein and lipid occurs in the fluid parts of the film at high pressure. All these studies reinforce the important role of SP-B in establishing and maintaining DPPC-rich layers for lung function.

CONCLUSION

NR results were used to calculate the molecular area of SP-B at the air/water interface as a function of surface pressure. From this information, we were able to obtain an independent determination of the concentration of the protein spreading solution. Mixing ratios for SP-B to DPPC were initially determined from isotherms of the pure solutions. The NR results indicate the mixture contains 46.2 DPPC molecules per SP-B molecule.

Analysis of the NR data for the mixtures showed the build-up of layers at the interface as the surface pressure was increased. With the range of contrasts used, these layers were assigned as a top layer of DPPC tails, a middle layer consisting predominantly of headgroups, and a region of SP-B excluded from the DPPC layer next to the subphase. This layer of SP-B remains closely associated with the DPPC layer.

The authors thank Professors Paul Kroon and Paul Masci for allowing us the use of their laboratories for the purification of the SP-B used in this work. The SP-B sequencing was performed by Katie Baldwin in the laboratory of Professor Paul Alewood. We also thank Karen Aberdeen, Dr Ben O'Driscoll, and Chris Wood for their assistance with associated work.

This work was supported by an Australian Synchrotron Research Program Fellowship (to W.K.F.) and the Access to Major Research Facilities Programme, which is a component of the International Science Linkages Programme established under the Australian Government's ''Backing Australia's Ability'' Innovation Statement.

REFERENCES

1. Beck, D. C., C.-L. Na, J. A. Whitsett, and T. E. Weaver. 2000. Ablation of a Critical Surfactant Protein B Intramolecular Disulfide Bond in Transgenic Mice. *J. Biol. Chem.* 275:3371–3376.
2. Lipp, M. M., K. Y. C. Lee, A. Waring, and J. A. Zasadzinski. 1997. Fluorescence, polarized fluorescence, and Brewster angle microscopy of palmitic acid and lung surfactant protein B monolayers. *Biophys. J.* 72:2783–2804.
3. Johansson, J., G. Nilsson, R. Stromberg, B. Robertson, H. Jornvall, and T. Curstedt. 1995. Secondary structure and biophysical activity of synthetic analogues of the pulmonary surfactant polypeptide SP-C. *Biochem. J.* 307:535–541.
4. Dieudonne, D., R. Mendelsohn, R. S. Farid, and C. R. Flach. 2001. Secondary structure in lung surfactant SP-B peptides: IR and CD studies of bulk and monolayer phases. *Biochim. Biophys. Acta.* 1511:99–112.
5. Lee, K. Y. C., J. Majewski, T. L. Kuhl, P. B. Howes, K. Kjaer, M. M. Lipp, A. J. Waring, J. A. Zasadzinski, and G. S. Smith. 2001. Synchrotron X-ray study of lung surfactant-specific protein SP-B in lipid monolayers. *Biophys. J.* 81:572–585.
6. Weaver, T. E., and J. J. Conkright. 2001. Functions of surfactant proteins B and C. *Annu. Rev. Physiol.* 63:555–578.
7. Wustneck, R., J. Perez-Gil, N. Wustneck, A. Cruz, V. B. Fainerman, and U. Pison. 2005. Interfacial properties of pulmonary surfactant layers. *Adv. Colloid Interface Sci.* 117:33–58.
8. Possmayer, F., K. Nag, K. Rodriguez, R. Qanbar, and S. Schurch. 2001. Surface activity in vitro: role of surfactant proteins. *Comp. Biochem. Physiol. A Mol. Integr. Physiol.* 129:209–220.
9. Oelberg, D. G., and F. Xu. 2000. Pulmonary surfactant proteins insert cation-permeable channels in planar bilayers. *Mol. Genet. Metab.* 70:295–300.
10. Crouch, E., and J. R. Wright. 2001. Surfactant proteins A and D and pulmonary host defense. *Annu. Rev. Physiol.* 63:521–554.
11. Nogee, L. M., G. Garnier, H. C. Dietz, L. Singer, A. M. Murphy, D. E. Demello, and H. R. Colten. 1994. A mutation in the surfactant protein-B gene responsible for fatal neonatal respiratory-disease in multiple kindreds. *J. Clin. Invest.* 93:1860–1863.
12. Tokieda, K., J. A. Whitsett, J. C. Clark, T. E. Weaver, K. Ikeda, K. B. McConnell, A. H. Jobe, M. Ikegami, and H. S. Iwamoto. 1997. Pulmonary dysfunction in neonatal SP-B-deficient mice. *Am. J. Physiol. Lung Cell. Mol. Physiol.* 17:L875–L882.
13. Zaltash, S., M. Palmblad, T. Curstedt, J. Johansson, and B. Persson. 2000. Pulmonary surfactant protein B: a structural model and a functional analogue. *Biochim. Biophys. Acta.* 1466:179–186.

14. Liepinsh, E., M. Andersson, J. M. Ruysschaert, and G. Otting. 1997. Saposin fold revealed by the NMR structure of NK-lysin. *Nat. Struct. Biol.* 4:793–795.

15. Putz, G., M. Walch, M. Van Eijk, and H. P. Haagsman. 1999. Hydrophobic lung surfactant proteins B and C remain associated with surface film during dynamic cyclic area changes. *Biochim. Biophys. Acta.* 1453:126–134.

16. Taneva, S., and K. M. W. Keough. 1994. Pulmonary surfactant proteins SP-B and SP-C in spread monolayers at the air-water interface. 1. Monolayers of pulmonary surfactant protein SP-B and phospholipids. *Biophys. J.* 66:1137–1148.

17. Cruz, A., L. Vazquez, M. Velez, and J. Perez-Gil. 2004. Effect of pulmonary surfactant protein SP-B on the micro- and nanostructure of phospholipid films. *Biophys. J.* 86:308–320.

18. Diemel, R. V., M. M. E. Snel, A. J. Waring, F. J. Walther, L. M. G. van Golde, G. Putz, H. P. Haagsman, and J. J. Batenburg. 2002. Multilayer formation upon compression of surfactant monolayers depends on protein concentration as well as lipid composition. *J. Biol. Chem.* 277:21179–21188.

19. Bringezu, F., J. Ding, G. Brezesinski, A. J. Waring, and J. A. Zasadzinski. 2002. Influence of pulmonary surfactant protein B on model lung surfactant monolayers. *Langmuir.* 18:2319–2325.

20. Follows, D., F. Tiberg, R. K. Thomas, and M. Larsson. 2007. Multilayers at the surface of solutions of exogenous lung surfactant: direct observation by neutron reflection. *Biochim. Biophys. Acta.* 1768:228–235.

21. Fullagar, W. K., K. A. Aberdeen, D. G. Bucknall, P. A. Kroon, and I. R. Gentle. 2003. Conformational changes in SP-B as a function of surface pressure. *Biophys. J.* 85:2624–2632.

22. Bünger, H., R.-P. Krüger, S. Pietschmann, N. Wüstneck, L. Kaufner, R. Tschiersch, and U. Pison. 2001. Two hydrophobic protein fractions of ovine pulmonary surfactant: isolation, characterization, and activity. *Protein Expr. Purif.* 23:319–327.

23. Penfold, J., R. C. Ward, and W. G. Williams. 1987. A time-of-flight neutron reflectometer for surface and interfacial studies. *J. Phys. E Sci. Instrum.* 20:1411–1417.

24. Brown, A. S., S. A. Holt, P. M. Saville, and J. W. White. 1997. Neutron and X-ray reflectometry: solid multilayers and crumpling films. *Aust. J. Chem.* 50:391–405.

25. Penfold, J., and R. K. Thomas. 1990. The application of the specular reflection of neutrons to the study of surfaces and interfaces. *J. Phys. Condens. Matter.* 2:1369–1412.

26. Braslau, A., P. S. Pershan, G. Swislow, B. M. Ocko, and J. Als-Nielsen. 1988. Capillary waves on the surface of simple liquids measured by x-ray reflectivity. *Phys. Rev. A.* 38:2457–2470.

27. Daillant, J., L. Bosio, B. Harzallah, and J. J. Benattar. 1991. Structural properties and elasticity of amphiphilics on water. *J. Phys. II.* 1:149–170.

28. Haagsman, H. P., and R. V. Diemel. 2001. Surfactant-associated proteins: functions and structural variation. *Comp. Biochem. Physiol. A Mol. Integr. Physiol.* 129:91–108.

29. Olafson, R. W., U. Rink, S. Kielland, S. H. Yu, J. Chung, P. G. Harding, and F. Possmayer. 1987. Protein sequence analysis studies on the low molecular weight hydrophobic proteins associated with bovine pulmonary surfactant. *Biochem. Biophys. Res. Commun.* 148:1406–1411.

30. Johansson, J., T. Curstedt, and H. Jornvall. 1991. Surfactant protein B: disulfide bridges, structural properties, and kringle similarities. *Biochemistry.* 30:6917–6921.

31. Oosterlaken-Dijksterhuis, M. A., H. P. Haagsman, L. M. G. Van Golde, and R. A. Demel. 1991. Characterization of lipid insertion into monomolecular layers mediated by lung surfactant proteins SP-B and SP-C. *Biochemistry.* 30:10965–10971.

32. Taneva, S. G., J. Stewart, L. Taylor, and K. M. W. Keough. 1998. Method of purification affects some interfacial properties of pulmonary surfactant proteins B and C and their mixtures with dipalmitoylphosphatidylcholine. *Biochim. Biophys. Acta.* 1370:138–150.

33. Krol, S., M. Ross, M. Sieber, S. Kunneke, H.-J. Galla, and A. Janshoff. 2000. Formation of three-dimensional protein-lipid aggregates in monolayer films induced by surfactant protein B. *Biophys. J.* 79: 904–918.

34. Naumann, C., T. Brumm, A. Rennie, J. Penfold, and T. M. Bayerl. 1995. Hydration of DPPC monolayers at the air/water interface and its modulation by the nonionic surfactant C12E4: a neutron reflection study. *Langmuir.* 11:3948–3952.

35. Pastrana-Rios, B., C. R. Flach, J. W. Brauner, A. J. Mautone, and R. Mendelsohn. 1994. A direct test of the ''squeeze-out'' hypothesis of lung surfactant function. External reflection FT-IR at the air/water interface. *Biochemistry.* 33:5121–5127.

36. Pastrana-Rios, B., S. Taneva, K. M. W. Keough, A. J. Mautone, and R. Mendelsohn. 1995. External reflection absorption infrared spectroscopy study of lung surfactant proteins SP-B and SP-C in phospholipid monolayers at the air/water interface. *Biophys. J.* 69: 2531–2540.